Sequential Open-Boundary Control by Data Assimilation in a Limited-Area Model

JIEPING ZOU* AND WILLIAM W. HSIEH

Department of Oceanography, University of British Columbia, Vancouver, British Columbia, Canada

I. M. NAVON

Department of Mathematics and SCRI, The Florida State University, Tallahassee, Florida

(Manuscript received 21 October 1994, in final form 6 March 1995)

ABSTRACT

The feasibility of sequential open-boundary control by data assimilation in a regional ocean model has been investigated using a barotropic wind-driven ocean circulation model. A simple open-boundary scheme has been constructed based on the idea of optimal boundary control of a diagnostic equation and illustrated with the problem of modeling the subpolar gyre subject to an open southern boundary. The results show that use of such a scheme in conjunction with traditional radiation boundary conditions allows for a longer model integration that would otherwise be unstable when only the radiation boundary conditions are imposed due to presence of dispersive waves.

1. Introduction

Any atmospheric or oceanic modeling short of global coverage encounters the open-boundary problem. Charney et al. (1950) were the first to address the open boundary problem in a finite-region weather forecasting model based on the barotropic vorticity equation. Along the open boundaries, the streamfunction (actually the geopotential) was specified. At "inflow" parts of the boundary, as indicated by the sign of the tangential gradient of the specified streamfunction, vorticity was also specified. This became a widely accepted approach, though Bennett and Kloeden (1978) and Miller and Bennett (1988) cautioned that the inflow vorticity advection boundary condition was not well posed. [For further discussions of initial boundary value problems in fluid dynamics, readers are referred to Oliger and Sundstrom (1978).]

Radiation boundary conditions (Orlanski 1976; Camerlengo and O'Brien 1980), well-known numerical algorithms for implementing the Sommerfeld radiating boundary condition, are designed to allow disturbances originated within the model domain to exit via the open boundary without disturbing the interior. The review paper by Roed and Cooper (1986) described further extensions to include obliquely incident waves and forced waves. While the radiation boundary conditions worked well for nondispersive waves, the application of these boundary conditions to systems that admit dispersive waves (e.g., Rossby waves for which the group velocity and phase velocity may be in drastically different directions) has encountered difficulties (e.g., Cummins and Mysak 1988). Consequently, modelers often turn to the sponge layers (i.e., regions of heavy damping) to prevent reflection into the model interior (Cummins and Mysak 1988), or to a one-way grid-nesting method where a coarse-grid model is matched to the finer-grid model along the open boundary (Robinson and Haidvogel 1980).

The advent of the optimal-control/adjoint-equations approach to oceanography in recent years (Thacker and Long 1988; Tziperman and Thacker 1989; Derber and Rosati 1989; Smedstad and O'Brien 1991; Yu and O'Brien 1991; Tziperman et al. 1992; Zou and Holloway 1995) prompted us to investigate open-boundary control (OBC) in limited-area ocean models from a data assimilation perspective. In fact, Thacker and Long (1988) have suggested this possibility, pointing out that open-boundary conditions are entirely analogous to initial conditions and forcing, and should be determined as part of fitting dynamics to data. Le Dimet (1988) formulated OBC in a general mathematical framework. Recently, Lardner (1992) carried out adjoint OBC for a depth-averaged tidal model by assimilating the data from tide gauges into the model interior. More recently, Ledimet and Ouberdous (1993a,b) have exercised OBC in their retrieval of

* Current affiliation: Supercomputer Computations Research Institute, The Florida State University, Tallahassee, Florida.

Corresponding author address: Dr. I. M. Navon, Dept. of Mathematics, The Florida State University, B-186, Tallahassee, FL 32306-4052.
E-mail: navon@scri.fsu.edu.

mass-balanced fields. With a limited-area shallow-water equations model, Zou et al. (1993) have examined the performance of variational data assimilation via both OBC and initial condition control (ICC) in relation to the performance via ICC only.

The idea of the adjoint OBC is to treat model variables along open boundaries as control variables and systematically adjust them through an iteration procedure until model outputs are optimally close to their observational counterparts. The closeness is assessed by a cost function J measuring misfit between data and model counterparts in a weighted norm. The optimality is accomplished by minimizing J with respect to the boundary values subject to some constraints.

In the usual adjoint OBC approach, the constraints consist of the whole set of model equations, leading to a set of adjoint model equations that are comparable with the model equation in terms of mathematical complexity. The dimension of resulting minimization problems for J is $O(MN)$ if boundary values are the only unknown parameters, where M is the number of boundary values to be determined at one time step and N the number of time steps required for a model integration. Consider a simple case where a regional model has only one side of its domain open along which only one dynamic variable needs to be specified at $M(=30)$ horizontal grid points for $N(=1000)$ time steps, the dimension of the control variables amounts to 30×1000. Thus, deducing boundary values from data in this way can be computationally intensive when a long integration period for a full size GCM is considered. It can also be difficult as seen in Zou et al. (1993) since the bound on the spectral condition number of Hessian of a cost function is proportional to $O[(MN)^{2/d}]$, where d is the number of space dimensions [provided that the operators originate in a discretization of an initial boundary value problem by either finite-element or finite-difference methods (Axelsson and Barker 1984; Axelsson 1994)]. One way to reduce the size of the optimization problem is to express boundary values at each boundary grid in terms of a sine series and truncate it at some level less than N(Seiler 1993). Physically, this amounts to filtering high-frequency variability along boundaries.

In this paper we describe a simple OBC scheme for which the size of the minimization problem is of order of $O(M)$. The reduction results from minimizing J subject only to diagnostic relations, as opposed to full-scale adjoint OBC where prognostic relations are also taken as constraints. The consequence of this choice of constraints is that our OBC scheme involves model/adjoint variables only at one time level, and hence it can readily be implemented whenever data is available during the course of model integration. This feature allows the scheme to be implemented with temporally interpolated data as often as required by accuracy considerations at intermediate time steps located between two consecutive data-arrival times. On the other hand, the same feature allows a number of numerical procedures including the radiation boundary conditions to be employed at non–data-arrival time steps, so that assimilation of temporally interpolated data can be reduced or eliminated, thus lowering computational cost. The simplicity and flexibility of this open-boundary control scheme are obtained at the expense of replacing a minimization that is globally optimal in time with one that is only locally optimal in time.

Section 2 describes the simple OBC for a limited-area wind-driven ocean circulation model. In section 3, the scheme is illustrated by modeling the subpolar gyre with an open southern boundary, followed by summary and discussion in section 4.

2. Sequential open-boundary control

a. Model equations

The ocean model used to study the feasibility of sequential OBC by data assimilation into its interior domain is the one describing barotropic wind-driven ocean circulation in a limited-area $\Delta\Omega$. The model dynamics are governed by the nondimensional vorticity equation (Bryan 1963; Veronis 1966):

$$\frac{\partial \zeta}{\partial t} + RJ(\psi, \zeta) + \frac{\partial \psi}{\partial x} = -\epsilon_b + \epsilon_h^2 \zeta + \text{curl}\tau \quad (1a)$$

$$\nabla^2 \psi = \zeta, \quad (1b)$$

which may be written in a discrete form

$$\zeta_{ij}^{n+1} = F(\zeta^n, \zeta^{n-1}, \psi^n, R, \epsilon_b, \epsilon_h, \tau), \quad (2a)$$

$$\nabla^2 \psi_{ij}^{n+1} = \zeta_{ij}^{n+1}, \quad (2b)$$

where ψ is the streamfunction, ζ the relative vorticity, $J(\psi, \zeta)$ the Jacobian of ψ and ζ, and curlτ the wind stress curl. The nondimensional numbers, R, ϵ_b, ϵ_h, are the Rossby number, and the bottom and horizontal frictional parameters, respectively. The superscripts n refer to time $t^n = n\Delta t$, whereas the subscripts i and j denote the grid point $(x_i, y_j) = (i\Delta x, j\Delta y)$, where Δt is the time step size and Δx and Δy are the grid size in the x and y directions, respectively. Finally, ∇^2 represents the five-point finite-difference Laplacian operator in 2D.

The ocean model employed here [i.e., (1)], albeit simple, has been a milestone in physical oceanography (Bryan 1963; Veronis 1966) and contains such salient features of large-scale wind-driven ocean circulation as western boundary currents, midlatitude eastward jet, and standing Rossby waves. Note that the same model was employed by Tziperman and Thacker (1989) to elucidate the optimal-control/adjoint-equations approach to studying the oceanic general circulation. For our purpose, more important is the fact that the streamfunction within the framework of the model dynamics is linearly proportional to the sea surface height, a quantity that is being measured by the on-going satel-

lite altimetry mission Topex/Poseidon (Wunsch 1992) and represents one of the most important upcoming datasets for ocean circulation study. Besides, the absence of baroclinicity in the model allows us to separate the present study from the issue of how to constrain the deep circulation with surface information such as sea surface altimetry, an issue which itself is under intense investigation (Haines 1991; Ezer and Mellor 1994; Smedstad and Fox 1994).

To determine the circulation in $\Delta\Omega$, it is necessary to specify the values of the streamfunction ψ along $\Delta\Gamma$, the boundary of $\Delta\Omega$,

$$\psi_{ij}^{n+1} = \psi_b^{n+1} \quad \text{for} \quad (x_i, y_j) \in \Delta\Gamma. \tag{3}$$

Also note that the vorticity ζ value along $\Delta\Gamma$ is required to evaluate the Arakawa Jacobian term at the grid points one grid interior from the boundary. Next, we shall present a data assimilation scheme whereby the boundary values of ψ (and correspondingly ζ) can be optimally estimated from the data. The meaning of optimality in our context will be clarified in later sections.

b. An OBC problem

Let $\hat{\psi}^{n+1}$ denote the streamfunction data available at some interior grid points. The objective is now to identify ψ_b, the boundary values of ψ, that render the resulting circulation ψ from the model (2) as close as possible to what the interior data suggest. The closeness is measured by a weighted cost function J

$$J(\psi_b) \equiv \sum_{ij} \frac{1}{2} w_{ij}[\psi_{ij}^{n+1}(\psi_b) - \hat{\psi}_{ij}^{n+1}]^2, \tag{4}$$

measuring the difference between the observational data $\hat{\psi}_{ij}^{n+1}$ and model counterpart ψ_{ij}^{n+1}, where w_{ij} is a weighting matrix taken to be the inverse of the error covariance matrix of the data $\hat{\psi}_{ij}^{n+1}$. The dependence of J on the control variables ψ_b lies in that ψ^{n+1} is obtained by solving (2b) subject to the boundary condition (3). With this measure, the OBC problem may be stated as follows: given the data $\hat{\psi}^{n+1}$ and the model-predicted vorticity ζ_{ij}^{n+1}, one identifies a boundary condition ψ_b^* that minimizes $J(\psi_b)$ under the constraints of the diagnostic relation (2b).

The effort to determine ψ_b^* from data in this way may fail because the model-predicted vorticity ζ^{n+1} at time t^{n+1} may be inconsistent with the vorticity underlying the data (i.e., $\nabla^2\zeta^{n+1}$). This could arise from a variety of error sources, including the inadequate specification of boundary streamfunction values in the absence of data (e.g., from applying radiation boundary conditions). To ensure the compatibility between ζ^{n+1} and ζ^{n+1} ($\equiv\nabla^2\psi^{n+1}$), the model-predicted vorticity ζ^{n+1} should be corrected by an amount $\delta\zeta^{n+1}$. Correspondingly, the streamfunction ψ_{ij}^{n+1} should be obtained from the corrected vorticity by solving

$$\nabla^2\psi_{ij}^{n+1} = \zeta_{ij}^{n+1} + \delta\zeta_{ij}^{n+1} \tag{5}$$

subject to (3). Note that the correction $\delta\zeta^{n+1}$ itself will be among the control variables to be estimated from the data. To this end, the OBC problem may be stated as

$$\text{minimize} \quad J(\psi_b^{n+1}, \delta\zeta_{ij}^{n+1}) \tag{6}$$

subject to (5), where ζ_{ij}^{n+1} is predicted by the prognostic model [i.e., (2a)]. Note that the idea of correcting a model performance through data assimilation may also be found in Derber (1989).

It is important to point out that only part of the model equations, more specifically the modified diagnostic relation (5), is employed in the above-stated OBC problem. This has a practical consequence; that is, the minimization problem involves control variables only at one time level rather than a time series of such variables as would be the case when the full set of model equations are used, thus reducing the dimension of the minimization problem. This in turn allows the OBC to be readily implemented whenever data arrive during the course of model integration. The flexibility and reduction in control variables are obtained at the expense of replacing an OBC that is optimal globally in time as in the case of usual adjoint OBC (e.g., LeDimet 1988) with the current one, which is optimal only locally in time. Also note that the streamfunction solved from (5) is a mixture of the dynamics underlying (2a) through ζ_{ij}^{n+1} and the data through the boundary value ψ_b^{n+1} and the vorticity correction $\delta\zeta_{ij}^{n+1}$.

c. Solution of the OBC problem

The strategy taken here to solve (6) is to employ a gradient-based descent algorithm (Navon and Legler 1987), with a gradient calculated using the adjoint technique (Le Dimet and Talagrand 1986; Talagrand and Courtier 1987; Thacker and Long 1988; Smedstad and O'Brien 1991; Zou and Holloway 1995). Following Thacker and Long (1988), we convert the constrained minimization (6) into an unconstrained one by introducing a Lagrangian function L

$$L(\psi_{ij}^{n+1}; \mu_{ij}^{n+1}; \psi_b^{n+1}, \delta\zeta_{ij}^{n+1}) = J + \sum_{ij} \mu_{ij}^{n+1}(\nabla^2\psi_{ij}^{n+1} - \zeta_{ij}^{n+1} - \delta\zeta_{ij}^{n+1}), \tag{7}$$

where μ_{ij}^{n+1} are Lagrange multipliers and the summation is taken over all the interior points of $\Delta\Omega$. The dependence of L on ψ_b^{n+1} results from evaluating $\nabla^2\psi_{ij}^{n+1}$ at the points one grid interior to the boundary $\Delta\Gamma$. The stationarity condition of L with respect to μ_{ij}^{n+1} recovers the constraint (5), whereas the condition $\partial L/\partial\psi_{ij}^{n+1} = 0$ yields the adjoint equation of the constraint (5):

$$\nabla^2\mu_{ij}^{n+1} = w_{ij}(\hat{\psi}_{ij}^{n+1} - \psi_{ij}^{n+1}) \tag{8}$$

$$\mu_{ij}^{n+1} = 0 \quad \text{for} \quad i, j \text{ on } \Delta\Gamma. \tag{9}$$

It is interesting to note that the adjoint equation is subject to a homogeneous boundary condition (9) despite

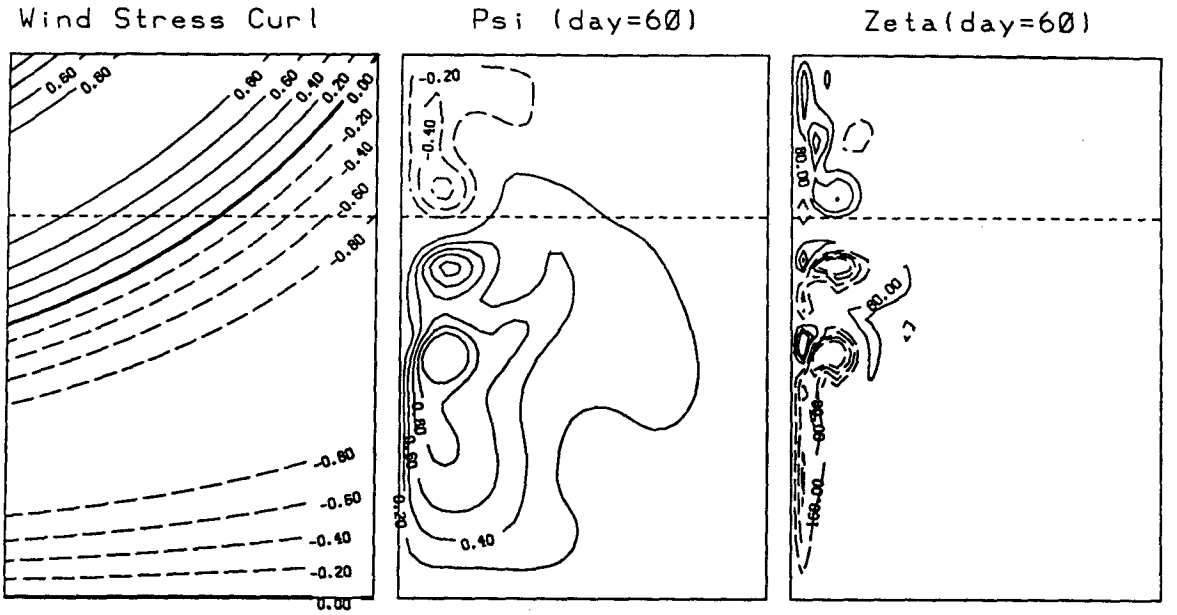

FIG. 1. (a) The steady wind stress curl used in this study. (b) The streamfunction ψ for the reference ocean at day 60, and (c) the corresponding relative vorticity ζ. The horizontal dashed line indicates the southern boundary of the subpolar gyre. All variables plotted in this and other figures are nondimensionalized variables.

the inhomogeneous nature of the boundary condition in its companion problem (5). Also note that it is the misfit between the data $\hat{\psi}_{ij}^{n+1}$ and the model counterpart ψ_{ij}^{n+1}, that is, the rhs of (8), that acts as a source function in the adjoint equation.

The gradient of J with respect to the control variables, ψ_b^{n+1} and $\delta\zeta_{ij}^{n+1}$, can then be expressed in terms of solutions to the adjoint equations,

$$\frac{\partial J}{\partial \psi_b^{n+1}} = \frac{\mu_{b-1}^{n+1}}{\Delta x \Delta y} \tag{10}$$

$$\frac{\partial J}{\partial \delta\zeta_{ij}^{n+1}} = -\mu_{ij}^{n+1}, \tag{11}$$

where μ_{b-1}^{n+1} denotes the values of μ at one grid interior to the boundary $\Delta\Gamma$, with Δx and Δy being the grid spacing in x and y, respectively.

With the gradient given by (10) and (11), the minimization of J can then be carried out with standard unconstrained minimization packages (Navon and Legler 1987; Zou et al. 1993), which typically involve an iteration procedure:

1) Set iteration count $m = 0$; make an initial guess at $\mathbf{u}^0$, a vector consisting of all the control variables ψ_b^{n+1} and $\delta\zeta_{ij}^{n+1}$; calculate $J(\mathbf{u}^0)$ from (4) by solving the constraint (5); and $\nabla J(\mathbf{u}^0)$ from (10) and (11) by solving the adjoint equation (8).

2) Set $m = m + 1$, check satisfaction of the iteration convergence criterion, and exit if it is satisfied or continue to next step if not.

3) Take one step in the descent direction $\mathbf{d}^m$ to update the control vector $\mathbf{u}^{m+1} = \mathbf{u}^m + \lambda^m \mathbf{d}^m$, where λ^m is the size of the step along $\mathbf{d}^m$.

4) Find out $J(\mathbf{u}^{m+1})$ and $\nabla J(\mathbf{u}^{m+1})$ as in step 1 but for the updated control variables $\mathbf{u}^{m+1}$, and go to step 2. The iteration continues until a prescribed convergence criterion is met.

To this end, implementing the OBC during the course of the model integration over a limited-area may proceed, possibly in conjunction with some existing open-boundary conditions (e.g., radiation boundary conditions), as follows:

(a) Advance the prognostic field to obtain ζ_{ij}^{n+1} by time stepping the prognostic equation (2a).

(b) If data are available for assimilation, solve the OBC problem (6) to deduce ψ_b^{n+1} (and, e.g., then calculate ζ_b^{n+1} by one-side difference approximation) and the interior vorticity correction $\delta\zeta_{ij}^{n+1}$. If no data is available, apply available open-boundary conditions (e.g., radiating boundary condition).

(c) Solve for the streamfunction from (5) (set $\delta\zeta_{ij}^{n+1} = 0$ in case of no data), with the boundary streamfunction values ψ_b^{n+1} determined either from the OBC or by other means.

Note that the OBC may be carried out with temporally interpolated data at intermediate time steps located between two consecutive data-arrival times. Clearly, this can be done as often as required by accuracy considerations or can be totally avoided to lower

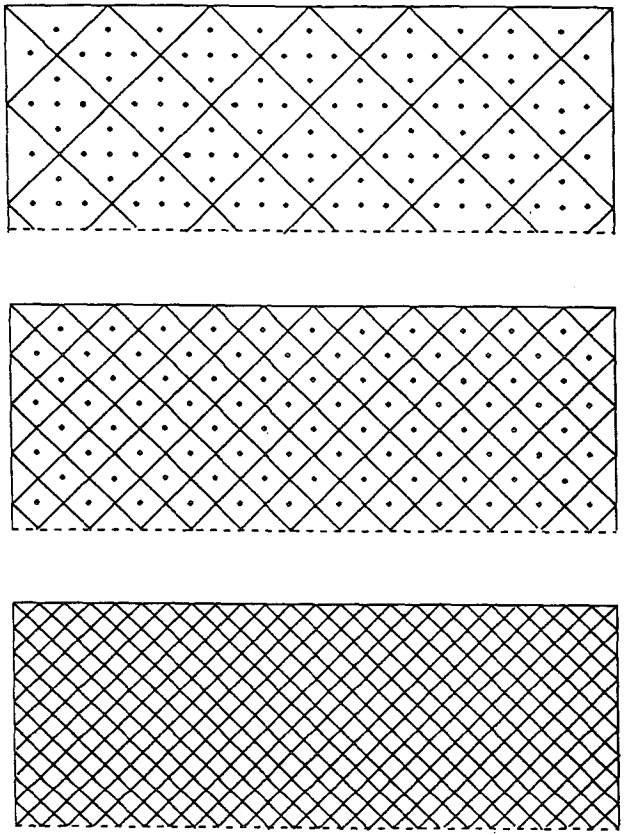

FIG. 2. Schematic arrangement of data points (the crossing points) in relation to the model grid (the dots) for the subpolar gyre region, where the diagonal lines represent ascending and descending satellite altimeter tracks and the dashed line the southern open boundary. (a) For the data points sampled every four grid points and at a 5-day repeat cycle, (b) for the data points sampled every two grid points and at a 10-day repeat cycle, (c) for the data points sampled every grid point and at a 20-day repeat cycle.

computational cost by resorting to radiation boundary conditions, for example.

3. Numerical illustration

a. Reference ocean and simulated data

We illustrate application of our OBC scheme with the problem of modeling the subpolar gyre subject to an open southern boundary. This experiment configuration, though idealized, bears on more realistic modeling efforts such as those carried out for the northeast Pacific by Hsieh (1987), Cummins and Mysak (1988), and Jiang et al. (1995). In these earlier studies, the southern open boundary was treated as a free-slip solid wall or a sponge layer (i.e., an excessive dissipation layer), which, for example, in the former case, resulted in noisy and unrealistic model behaviors near the southern open boundary. Hopefully, implementation of the OBC scheme in our simple problem may shed some light on the issue of the southern open boundary in these regional modeling efforts. Also, it is desirable to carry out such an effort with simulated data so that one can assess its performance against the "true solution."

A reference ocean consisting of wind-driven double gyres was set up in a closed basin with a 33×65 grid. The nondimensional parameters used are $R \equiv \tau_0/\rho D\beta^2 L^3 = 1.26 \times 10^{-3}/2\pi$, $\epsilon_h \equiv \kappa_h/\beta L^3 = 1.6 \times 10^{-5}$, and $\epsilon_b = \kappa_b/\beta L = 0$, where wind stress $\tau_0 = 0.5$ N m^{-2}, density $\rho = 10^3$ kg m^{-3}, depth $D = 400$ m, planetary beta $\beta = 2 \times 10^{-11}$ m^{-1} s^{-1}, zonal length $L = 2500$ km, meridional length of $2L$, lateral diffusion coefficient $\kappa_h = 5 \times 10^3$ m^2 s^{-1}, bottom friction coefficient $\kappa_b = 0$. The reference ocean, forced by the asymmetric wind stress curl $\sin[\pi(1 - x)y/2]$ shown in Fig. 1a, was well spun up by day 60 (Fig. 1) and was then extended for a few more months, featuring such facets of large-scale wind-driven ocean circulation as intense currents of order $O(1.0$ m s$^{-1})$ near the western boundary, broad southward Sverdrup-type flow of order $O(0.05$ m s$^{-1})$ in the interior, and a subpolar gyre centered in the northwest. Of the dynamical processes that have direct impact on the performance of the OBC scheme are the boundary separation current running northeastward and the recirculation in both gyres. The strength of these dynamical features fluctuates, and their locations shift up and down the west boundary, corresponding to the dominant basin Rossby mode, which is found to have a period of approximately 15 days for the parameter used here. [In real oceans with larger domains, this dominant basin mode would have a longer period (LeBlond and Mysak 1978, 299–301).]

During the extended integration, streamfunction data were sampled every four grid points over the subpolar gyre and at a 5-day repeat cycle as schematically shown in Fig. 2a. The spatial and temporal resolutions of this sampling roughly correspond to those attained for the subpolar gyre region by a near polar-orbiting satellite altimeter at an altitude of around 800 km. Of course the satellite altimeter would offer a far denser sampling along satellite tracks. During the extended run, data were also collected every two grid points and at a 10-day repeat cycle (Fig. 2b) as well as every grid point and at a 20-day repeat cycle (Fig. 2c), yielding datasets with increasing spatial resolution but decreasing temporal resolution.

b. Results

Four model integrations were carried out for the subpolar region with its southern boundary open as marked by the dashed line in Fig. 1. The runs were initialized with the state of the reference run at day 60. The data collected with the 5-day repeat cycle from the extended reference run were assimilated into this subdomain to carry out the OBC. In between the repeated assimilations—that is, during the nonassimilation time steps—

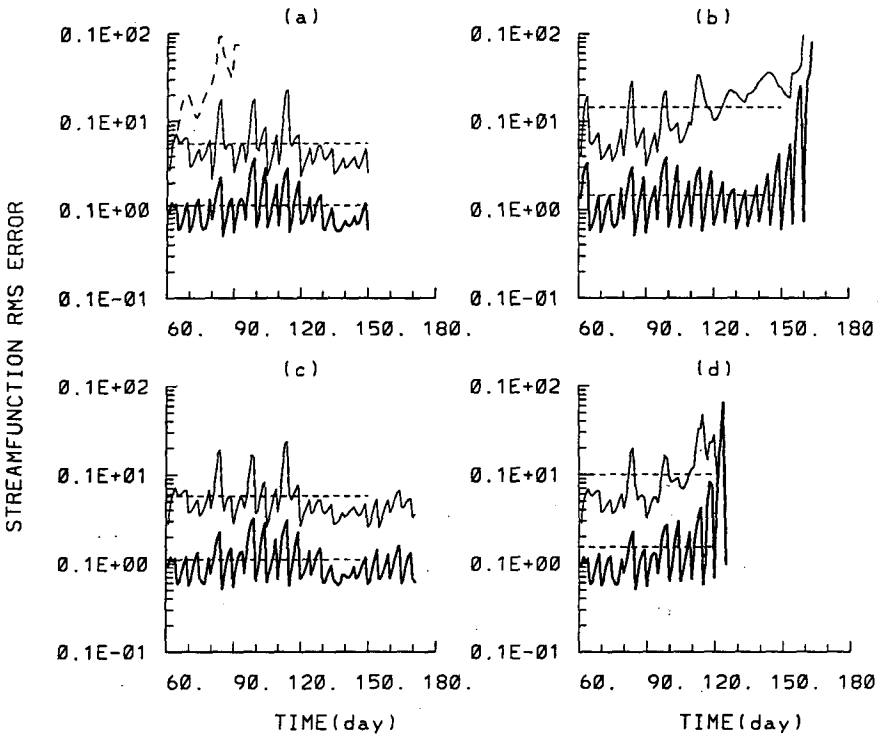

FIG. 3. The streamfunction rms errors over the subpolar domain excluding the southern open boundary (thick curves) and the rms error along the open boundary (thin curves) for experiments I through IV, respectively. The dashed horizontal lines indicate the time-averaged rms error over the duration covered by the line. The dashed curve in (a) corresponds to a run where no OBC was performed and radiation boundary conditions were applied to both ψ and ζ. Experiment IV eventually blew up, hence curves are displayed for a shorter duration. (See section 3b for description of experiments I–IV.)

the open southern boundary condition was varied in the four experiments: (I) the radiation boundary condition was applied to both the boundary streamfunction ψ_b and vorticity ζ_b, (II) both ψ_b and ζ_b were held constant (until the next assimilation time step when the OBC would assign new boundary values), (III) radiation boundary conditions was applied to ζ_b, but with ψ_b being held constant, and (IV) radiation boundary condition was applied to ψ_b, but with ζ_b being held constant.

Root-mean-square (rms) error is employed as a measure of the performance of the OBC in the four experiments, which is defined, say for ψ, by $[\Sigma\ (\psi - \psi_{\text{ref}})^2]^{1/2}(\Sigma\ \psi_{\text{ref}}^2)^{-1/2}$, where ψ_{ref} denotes the streamfunctions in the reference run. Note that an rms error in ψ corresponds exactly to an error in sea surface height h since $h = (g/f_0)\psi$ within the quasigeostrophic dynamics, where f_0 is the reference value of the Coriolis parameter and g the gravity. It is seen in Fig. 3 that the rms error in ψ displays a sharp decline when the OBC by data assimilation is performed every 5 days. The horizontal dashed lines indicate the time-averaged rms errors. With both experiments I and III, the rms error remained well under control (with an average error of about 11% in ψ or equivalently in h), whereas for experiment II and IV, the error eventually skyrocketed in the time interval between data assimilations. [As experiment IV actually exploded around day 130, it was not pursued any further.] The error resulting from applying only the radiation boundary condition but without the OBC is shown as the dashed curve in Fig. 3a, displaying a rapid climb. Hence the OBC by data assimilation turned out to be crucial in keeping the rms error under control.

The vorticity rms errors are shown in Fig. 4, with an average error of about 35% for both experiments I and III, but with a gradually rising error trend in experiment II. The rather larger rms vorticity errors, compared to the rms streamfunction errors, are mainly due to the fact that the cost function J in (4) does not contain a term measuring departure of the model vorticity from observed vorticity. In fact, during an assimilation (or OBC) time step, vorticity is overadjusted to minimize the cost function, which reduces the streamfunction rms error (Fig. 3) but induces a rise in the vorticity rms error (Fig. 4). After the assimilation time step, the vorticity calculated from the prognostic equation (2a) gradually eliminates the overadjustment, leading to the

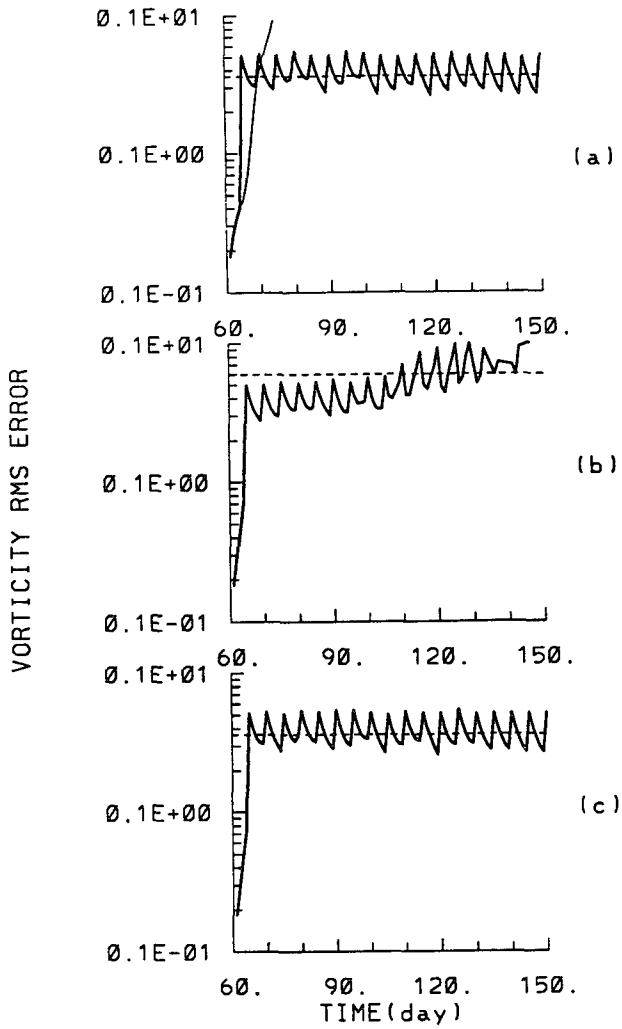

FIG. 4. Root-mean-square error of the relative vorticity in the subpolar gyre (excluding the open boundary) for experiments I–III. The dashed curves indicate the time-averaged rms errors. The thin curve in (a) displays the run without OBC.

drop in the vorticity rms error seen in Fig. 4. The rms errors in the total kinetic energy display poor behavior in experiment II but a good performance in experiments I and III where the average error is just above 10% (see Fig. 5).

Overall, the OBC in conjunction with the radiation boundary condition renders longer integration, which would otherwise be unstable with the radiation boundary condition alone. Of the four OBC experiments, experiment I (where the radiation boundary condition was applied to both ψ and ζ at nonassimilation time steps) yielded the best results.

To gain some physical insight into the OBC performance observed above, let us now focus on experiment I. Figures 6–8 show three solutions of the OBC problem (6) for this experiment at days 90, 120, and 150, with Fig. 6 displaying the streamfunction along the southern open boundary at these times, Fig. 7 the streamfunction for the subpolar domain, and Fig. 8 the vorticity correction. These solutions were obtained using the TNPACK (truncated Newton package) (Schlick and Fogelson 1992) algorithm, which typically converged within 10 iterations.

The close agreement (as seen in Fig. 6) between the OBC calculation and the reference values in the interior of the ocean may be anticipated from the fact that vorticity in the interior is essentially determined by the wind stress input, a constant field well defined throughout the computation domain in the present study. So there is little error in predicted vorticity ζ^{n+1} in the interior ocean (see Fig. 8), which renders it easier to solve the OBC problem (6) there. On the other hand, vorticity dynamics near the western boundary and re-

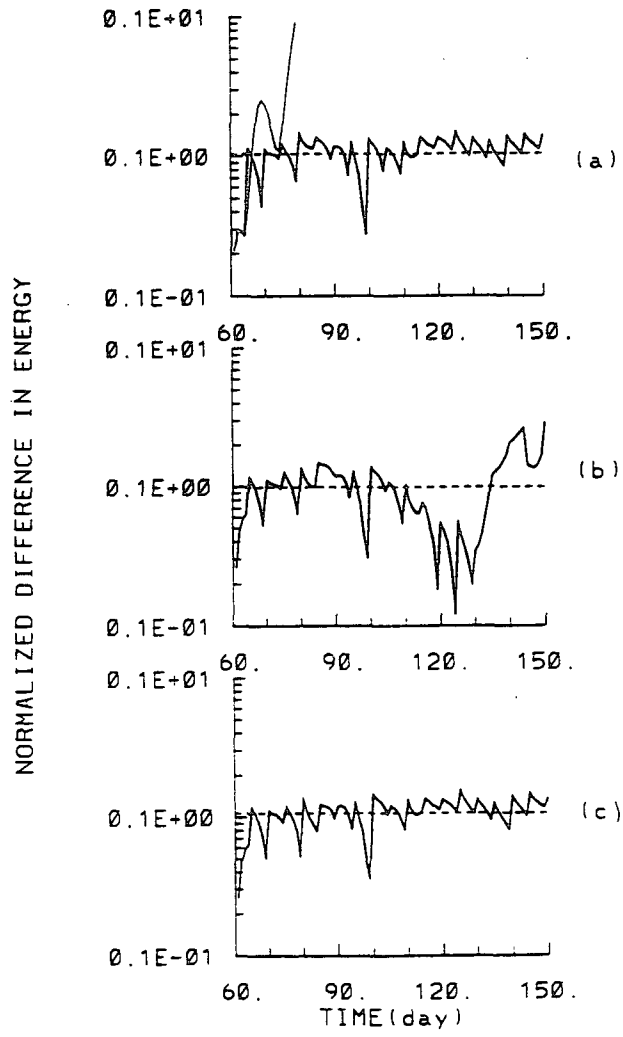

FIG. 5. Root-mean-square error of the total kinetic energy in the subpolar gyre for experiments I–III. The dashed curves indicate the time-averaged rms errors. The thin curve in (a) displays the run without OBC.

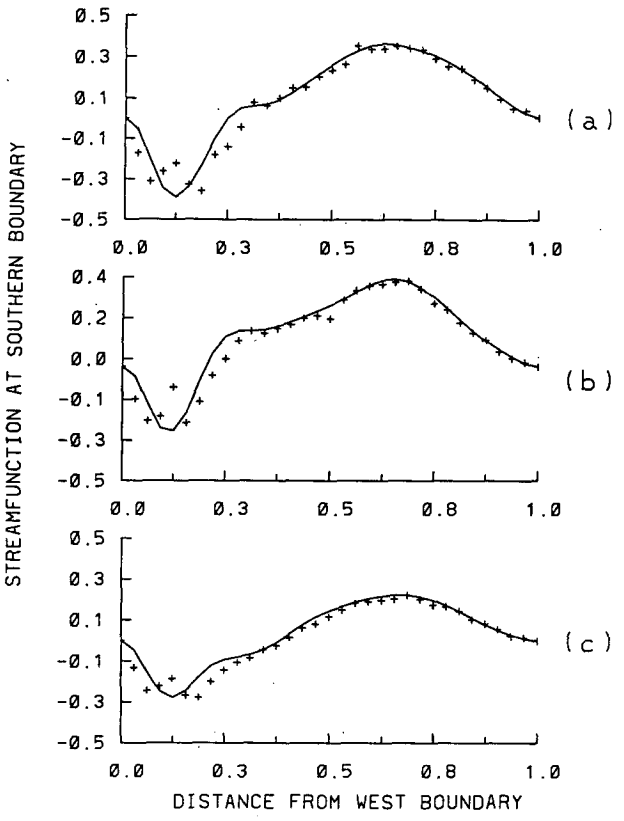

FIG. 6. Streamfunction along the open southern boundary as obtained from the OBC at (a) day 90, (b) day 120, and (c) day 150 for experiment I (indicated by the crosses). The curve displays the corresponding values from the reference ocean.

circulation regions is dominated by strong advective and diffusive processes associated with the western boundary currents and the separation current (see Figs. 7 and 8) for which the radiation boundary condition has limited skill to deal with (Cummins and Mysak 1988). Thus, the use of such boundary conditions during non-OBC time steps can result in considerable vorticity errors in those regions (Fig. 8). Part of the accumulated errors are removed by the vorticity correction (which turns out to be of almost the same order magnitude as ζ itself) (Fig. 8). The remainder of the errors manifest themselves in the inferred streamfunction in the vicinity of these locations.

Recall that the rms error around day 150 is generally smaller than the rms error around either day 90 or day 120 (cf. Fig. 3a). This is consistent with Fig. 7 in that of the three days, the OBC performs best at day 150. A physical reason for this may be that the separation current, advecting and diffusing positive vorticity from the subtropic gyre into the subpolar domain, is much weaker around day 150 (see Fig. 7), which does not test the limited ability of the radiation boundary condition as severely. This together with Fig. 6 suggests that in order to optimize the OBC performance, the location of an open boundary should be as far away as possible from dynamically active regions.

The large features in the reference ocean are well captured in the corresponding assimilated ocean (see Figs. 6 and 7). This implies that errors in the latter (as might be seen by taking the difference between the left column and the right column in Fig. 7) reside essentially on the grid size scale. Also, Fig. 7 shows that a large number of the errors occurs near the open boundary, in agreement with our earlier observation (from Fig. 3) that rms error in ψ is far larger along the open boundary than in the interior.

Some extra runs were carried out to assess the impact that dynamical variability of the reference ocean may have on the choice of the required frequency of carrying out the OBC. We tried the OBC with the dataset collected every other grid point and at a 10-day repeat cycle (cf. Fig. 2b). With this denser data coverage, the rms error was reduced more at OBC time steps than in the 5-day assimilation cases; however, the longer time interval without OBC application in these runs led to time-averaged rms errors significantly higher than those in the 5-day assimilation runs. We also carried out the OBC with the dataset collected at every grid point and at a 20-day repeat cycle (cf. Fig. 2c), which yielded even larger time-averaged rms errors. Thus, the denser spatial coverage was not able to compensate for the coarser time coverage in our OBC. A variant of the 5-day repeat cycle experiment was also performed, where two subsequent data fields were interpolated to yield a data field at the intermediate time. The resulting rms errors were smaller than in the 5-day assimilation runs, suggesting that more frequent OBC with temporally interpolated datasets would yield further improvements. Recall that the reference ocean has variability associated with the first barotropic mode of period of approximately 15 days. Thus, the OBC should be carried out not less than a few times over one period of dominant variability in order to achieve its desired performance.

4. Summary and discussion

A barotropic wind-driven ocean circulation model has been employed to examine the feasibility of open-boundary control by sequential data assimilation. A simple sequential OBC has been constructed based on the idea of optimal boundary control of diagnostic relation by data assimilation. Its performance has been examined for solving the problem of modeling the subpolar gyre. The results obtained have shown that the OBC in conjunction with radiation boundary conditions renders longer time integration that would be unstable with radiation boundary conditions alone due to presence of dispersive waves.

We have made an exploratory investigation of sequential OBC by data assimilation for a limited-area model. A host of questions can and should be raised.

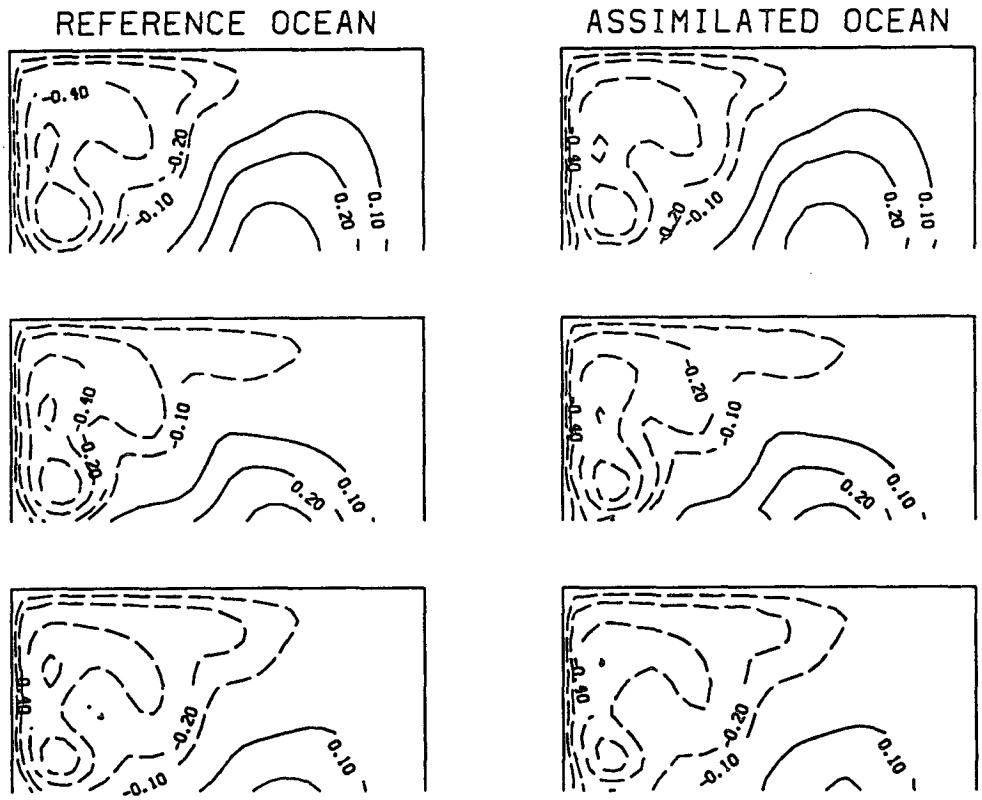

FIG. 7. Streamfunction for the subpolar gyre region. The left column is from the reference ocean, and the right column from experiment I at day 90 (top panels), day 120 (middle panels), and day 150 (bottom panels).

We shall conclude by mentioning some of the broader issues.

OBC with usual adjoint approach (Le Dimet 1988; Lardner 1992; Zou et al. 1993) would involve estimation of a time series of boundary values over a time period of a model integration. In the case of an oceanic climate study, the timescale involved can be of order of decades or even longer and thus dictate model integration over a time period of the same length as the timescale concerned. In that case, a storage of a complete nonlinear trajectory as required by a backward adjoint integration is quite impossible with present computer resources. More importantly, the tangent linear model and its adjoint may become invalid over such an extended time period (Gauthier 1992). Clearly, these concerns are absent with sequential OBC as performed here. It is important to point out, though, that this very advantage of the sequential OBC is achieved at the loss of global optimality in time for the estimated boundary values. Moreover, there are a number of important considerations to take into account in the case of sequential OBC as well, among which is how frequently to carry out the OBC and where to optimally locate an open boundary (cf. section 3b).

Sequential OBC has been discussed here for regional modeling of time-dependent flows. The same idea may also apply to steady-state problems as in Le Dimet and Ouberdous (1993a) where they performed OBC for the nonlinear balance equation to retrieve mass-balanced geopotential and streamfunction fields. In this regard, sequential OBC may be viewed as a spatial interpolation scheme for sparse data while respecting some aspects of model dynamics, and thus analogous to optimal interpolation.

Within the quasigeostrophic dynamics, streamfunction is linearly related to sea surface displacement. The effectiveness of the OBC with the simulated streamfunction data as seen in the last section suggests potential usefulness of satellite altimetry data for OBC in limited-area models. It should be pointed out though that our illustrations with the simulated data have a number of unrealistic features compared to real altimeter data. For example, it was assumed that all the data were available at one instant, whereas in reality altimetry data are sampled along tracks and continuously over several days. Clearly, future work needs to examine how to model accumulation of altimetry data over a repeat cycle more realistically and to appropriately interpolate the data in time and space for better assimilation.

Finally, it should be emphasized that the favorable comparison of the retrieved open-boundary conditions

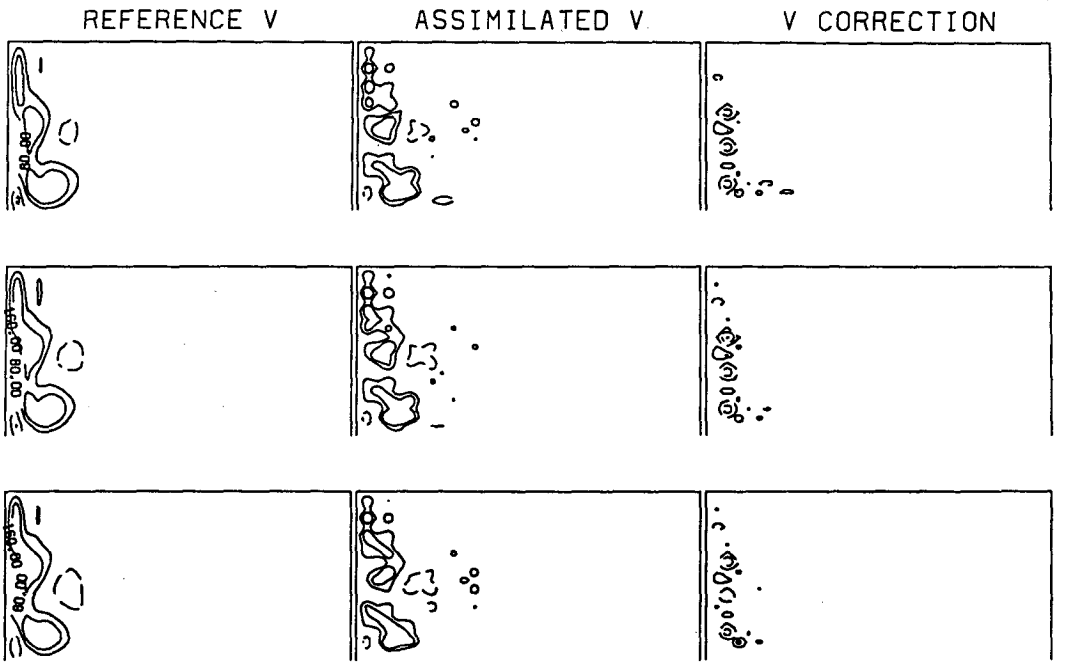

FIG. 8. Relative vorticity for the subpolar gyre region. The left column is from the reference ocean, the middle column from experiment I at day 90 (top panels), day 120 (middle panels), and day 150 (bottom panels). The right column is for the vorticity correction $\delta\zeta$ obtained from the OBC at the corresponding times.

with the reference ocean as shown in section 3 is obtained with an idealized wind-driven ocean model [cf. (1)]. On the other hand, we do not see any obvious reason why the OBC should fail in more realistic situations where baroclinicity and mesoscale variability are present. In fact, the sequential OBC has been applied to midocean mesoscale eddy field [with its four sides open] by Bailey (1993), yielding desired results. Of course, in the presence of baroclinicity, one has to confront the issue of how to constrain the deep circulation with surface information (e.g., sea surface altimeter data), a subject that itself is under intense investigations (Ezer and Mellor 1994; Smedstad and Fox 1994). Also, one has to decide which diagnostic relations are to be open-boundary controlled. In the case of quasigeostrophic layer models (e.g., Cummins and Mysak 1988), for example, a natural choice is the relation between potential vorticity and streamfunction for each layer, which constitutes a direct extension from the present barotropic model.

Acknowledgments. This research was funded by the Natural Sciences and Engineering Research Council of Canada via the Canadian WOCE project and operating grants to W. Hsieh. Additional support was provided by NSF Grant ATM-9413050 managed by Dr. Pamela Stephens, and by the Supercomputer Computations Research Institute at The Florida State University, which was partially funded by the Department of Energy through Contract DE-FC0583ER250000.

REFERENCES

Axelsson, O., 1994: *Iterative Solution Methods.* Cambridge University Press, 654 pp.

——, and V. A. Barker, 1984: *Finite Element Solution of Boundary Value Problems.* Academic Press, 432 pp.

Bailey, D. A., 1993: Adjoint data assimilation in an open ocean barotropic quasi-geostrophic model. M.S. thesis, Oceanography Dept., University British Columbia, 51 pp.

Bennett, A. F., and P. E. Kloeden, 1978: Boundary conditions for limited-area forecasts. *J. Atmos. Sci.,* **35,** 990–996.

Bryan, K., 1963: A numerical investigation of a nonlinear model of a wind-driven ocean. *J. Atmos. Sci.,* **20,** 594–263.

Camerlengo, A. L., and J. J. O'Brien, 1980: Open boundary conditions in rotating fluids. *J. Comput. Phys.,* **35,** 12–35.

Charney, J. G., R. Fjortoft, and J. von Neumann, 1950: Numerical integration of the barotropic vorticity equation. *Tellus,* **2,** 237–254.

Cummins, P. F., and L. A. Mysak, 1988: A quasi-geostrophic circulation model of the northeast Pacific. Part I: A preliminary numerical experiment. *J. Phys. Oceanogr.,* **18,** 1261–1286.

Derber, J., 1989: A variational continuous assimilation technique. *Mon. Wea. Rev.,* **117,** 2437–2446.

——, and A. Rosati, 1989: A global oceanic data assimilation system. *J. Phys. Oceanogr.,* **19,** 1333–1347.

Ezer, T., and G. L. Mellor, 1994: Continuous assimilation of Geosat altimetry data into a three-dimensional primitive equation Gulf Stream model. *J. Phys. Oceanogr.,* **24,** 832–847.

Haines, K., 1991: A direct method for assimilating sea surface height data into ocean model with adjustments to the deep circulation. *J. Phys. Oceanogr.,* **21,** 843–868.

Hsieh, W. W., 1987: A numerical study of the seasonal cycle in the northeast Pacific Ocean as driven by the wind stress and surface heat flux. *Atmos.–Ocean,* **25,** 375–386.

Jiang, L., W. W. Hsieh, and P. F. Cummins, 1995: Assimilation of Geosat altimetric data into a quasi-geostrophic model of the sub-Arctic Pacific Ocean. *Atmos.–Ocean,* submitted.

Lardner, R. W., 1992: Optimal control of open boundary conditions for a numerical tidal model. *Comput. Meth. Appl. Meth. Eng.*, **102,** 367.

Leblond, P. H., and L. A. Mysak, 1979: *Waves in the Oceans.* Elsevier, 602 pp.

Le Dimet, F. X., 1988: Determination of the adjoint of a numerical weather prediction model. Tech. Rep. FSU-SCRI-88-79, The Florida State University, Tallahassee, FL, 22 pp. [Available from SCRI, FSU, Tallahassee, FL, 32306.]

——, and O. Talagrand, 1986: Variational algorithms for analysis and assimilation of meteorological observations: Theoretical aspects. *Tellus,* **38A,** 97–110.

——, and M. Ouberdous, 1993a: Retrieval of balanced fields: An optimal control technique. *Tellus,* **45A,** 449–461.

——, and ——, 1993b: Optimal control and data assimilation. *Mathematics and Climate,* J. L. Lions and J. Diaz, Eds., Masson, 320 pp.

Miller, R. N., and A. F. Bennett, 1988: Numerical simulation of flows with locally characteristic boundaries. *Tellus,* **40A,** 303–323.

Navon, I. M., and D. M. Legler, 1987: Conjugate-gradient methods for large-scale minimization in meteorology. *Mon. Wea. Rev.*, **115,** 1479–1502.

Oliger, J., and A. Sundstrom, 1978: Theoretical and practical aspects of some initial boundary value problems in fluid dynamics. *SIAM J. Appl. Math.*, **35,** 419–446.

Orlanski, I., 1976: A simple boundary condition for unbounded hyperbolic flows. *J. Comput. Phys.*, **21,** 251–269.

Robinson, A. R., and D. B. Haidvogel, 1980: Dynamical forecast experiments with a barotropic open ocean model. *J. Phys. Oceanogr.*, **10,** 1909–1928.

Roed, L. P., and C. K. Cooper, 1986: Open boundary conditions in numerical ocean models. *Advanced Physical Oceanographic Numerical Modeling,* J. J. O'Brien, Ed., Reidel, 411–436.

Schlick, T., and A. Fogelson, 1992: TNPACK—A truncated Newton minimization package for large-scale problems. Part I: Algorithm and usage. Part II: Implementation examples. *ACM Trans. Math. Software,* **18,** 46–111.

Seiler, U., 1993: Estimation of open boundary conditions by the adjoint method. *J. Geophys. Res.*, **98,** 22 855–22 870.

Smedstad, O. M., and J. J. O'Brien, 1991: Variational data assimilation and parameter estimation in an equatorial pacific ocean model. *Progress in Oceanography,* Vol. 20, Pergamon, 672–688.

——, and D. N. Fox, 1994: Assimilation of altimeter data in a two-layer primitive equation model of the Gulf Stream. *J. Phys. Oceanogr.*, **24,** 305–325.

Talagrand, O., and P. Courtier, 1987: Variational assimilation of meteorological observations with the adjoint vorticity equation. Part I: Theory. *Quart. J. Roy. Meteor. Soc.*, **113,** 1311–1328.

Thacker, W. C., and R. B. Long, 1988: Fitting dynamics to data. *J. Geophys. Res.*, **93**(C2), 1227–1240.

Tziperman, E., and W. C. Thacker, 1989: An optimal-control/adjoint-equations approach to studying the oceanic general circulation. *J. Phys. Oceanogr.*, **19,** 1471–1485.

——, ——, R. B. Long, S. M. Hwang, and S. R. Rintoul, 1992: Oceanic data analysis using a general circulation model. Part II: A North Atlantic model. *J. Phys. Oceanogr.*, **22,** 1434–1457.

Veronis, G., 1966: Wind-driven ocean circulation. Part 2: Numerical solutions of the nonlinear problem. *Deep-Sea Res.*, **13,** 17–29.

Wunsch, C., 1992: Observing ocean circulation from space. *Oceanus,* **35,** 9–17.

Yu, L., and J. J. O'Brien, 1991: Variational estimation of the wind stress drag coefficient and the oceanic eddy viscosity profile. *J. Phys. Oceanogr.*, **21,** 709–719.

Zou, J., and G. Holloway, 1995: Improving steady-state fit of dynamics to data using adjoint equation with gradient preconditioning. *Mon. Wea. Rev.*, **123,** 199–211.

Zou, X., I. M. Navon, M. Berger, M. K. Phua, T. Schlick, and F. X. Le Dimet, 1993: Numerical experience with limited-memory, quasi-Newton methods for large-scale unconstrained nonlinear minimization. *SIAM J. Optimization,* **3,** 582–608.